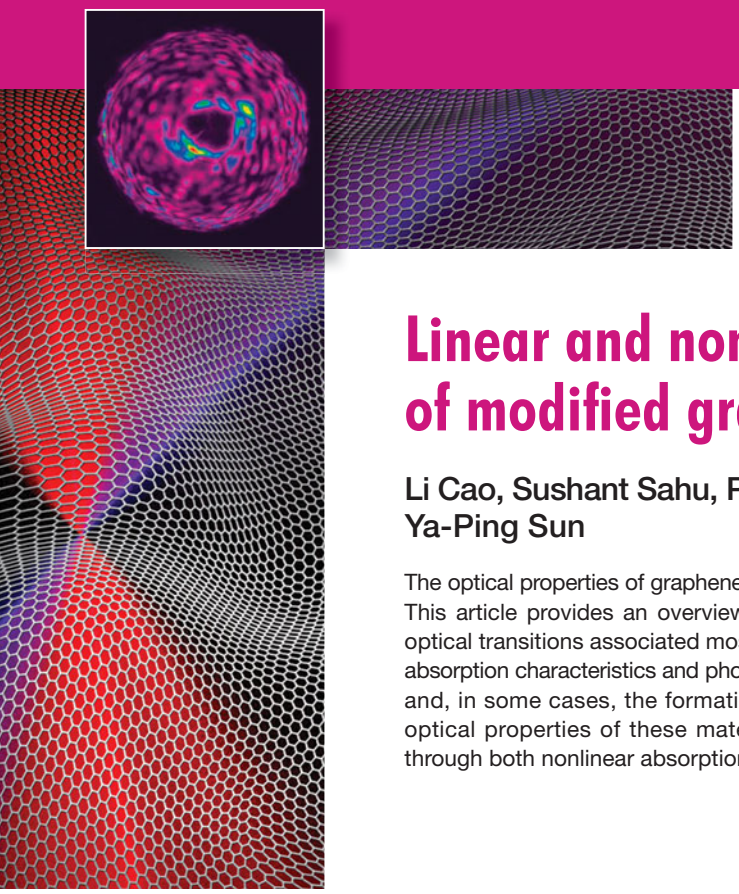


Linear and nonlinear optical properties of modified graphene-based materials

Li Cao, Sushant Sahu, Parambath Anilkumar, Chang Yi Kong, and Ya-Ping Sun

The optical properties of graphene-based nanomaterials have attracted much recent attention. This article provides an overview of recent advances in the study of linear and nonlinear optical transitions associated mostly with tailored energy bandgaps. In particular, the optical absorption characteristics and photoluminescence emissions due to various induced bandgaps and, in some cases, the formation of graphene quantum dots are highlighted. Nonlinear optical properties of these materials are reviewed with an emphasis on optical limiting through both nonlinear absorption and scattering mechanisms.

Introduction

Graphene, as a two-dimensional nanoscale sheet with an extended sp^2 carbon network, has attracted much recent attention for both fundamental investigations and potential technological applications.[1–7] The optical properties of graphene and related carbon nanomaterials and nanocomposites have also been widely explored.[8–14] Graphene sheets are generally produced either top-down by exfoliation of graphite,[12,15–17] including an indirect route through oxidation into exfoliated graphene oxides (GOs) followed by reduction,[12,17] or bottom-up by techniques such as vapor deposition.[18,19] Pristine graphene is a zero-bandgap material, but to manipulate and control its optical and electronic properties, researchers have devoted much effort to producing non-zero bandgaps.[20–23] Various approaches for opening energy gaps have been used in graphene materials by creating either defects or isolated nanoscale islands of graphene-like material.[9,22,24–31] These approaches can be separated into two categories, depending on whether this modification is achieved by manipulating the π-electronic network to form sp^2 domains in a graphene sample or breaking large graphene sheets into nanoscale pieces.

Linear and nonlinear optical properties of graphene-based materials offer the potential for highly attractive applications in photonics and optoelectronics.[9,10,14,32,33] For example, photoluminescence associated with induced bandgaps in graphene has been pursued as an alternative to fluorescent quantum dots (QDs). In addition, because of its extended π network, graphene exhibits an excellent nonlinear optical reponse.[34–36] Among the various nonlinear optical properties of graphene materials, one of the most widely pursued has been optical limiting, which is important in a number of technologies, from passive manipulation of optical beams[35,37–39] to protection against intense laser pulses.[38] In this article, the optical absorption characteristics and photoluminescence properties due to various induced energy gaps and, in some cases, the creation of graphene quantum dots (GQDs) in graphene-based materials are highlighted. Nonlinear optical properties of these materials are reviewed with an emphasis on optical limiting through both nonlinear absorption and scattering mechanisms.

Absorption

Graphene sheets with sp^2-hybridized carbon atoms and associated π networks exhibit optical absorption over a broad spectral range from the ultraviolet to the near-infrared, although their insolubility has made solution-phase studies of optical absorption difficult.[17,22,28,40–42] As with other carbon nanomaterials, including carbon nanotubes and even carbon nanoparticles,[43–47] π-plasmon absorption plays a major role in photon harvesting by graphene-based materials.[9,48,49]

Graphene oxides (GOs) are graphene "derivatives" in which a substantial fraction of the sp^2-hybridized carbons are

Li Cao, Department of Chemistry, Clemson University; lcao@clemson.edu
Sushant Sahu, Department of Chemistry, Clemson University; sushans@clemson.edu
Parambath Anilkumar, Department of Chemistry, Clemson University; p.anilkumar@live.in
Chang Yi Kong, Department of Chemistry, Clemson University; ckong@clemson.edu
Ya-Ping Sun, Department of Chemistry, Clemson University; syaping@clemson.edu
DOI: 10.1557/mrs.2012.178

© 2012 Materials Research Society

https://doi.org/10.1557/mrs.2012.178 Published online by Cambridge University Press

converted to sp^3 hybridization (up to 60% according to Ruoff and coworkers)[50] upon typically harsh oxidative treatment such as the Hummers method.[51] Aqueous suspensions of GOs (solution-like, **Figure 1**a) are readily prepared to allow quantitative optical absorption measurements.[17,40,52] The solubilized GOs (with primarily single-layer sheets) also serve as excellent precursors in various conversion schemes for the preparation of graphene sheets containing different ratios (purposely or by default) of sp^2 and sp^3 carbons.[22,53] As a typical example, gradual changes in optical absorption can be used to monitor the transformation of a GO film at various stages of reduction (by hydrazine, in the case of Figure 1b).[22] The same strategy was applied to follow the conversion of GOs in a thermal treatment in supercritical fluids at relatively low temperatures.[52]

Many other methods of altering the ratios between sp^2 and sp^3 carbons have been explored, including the formation of isolated sp^2 islands in graphene sheets and/or the manipulation of defects (associated with sp^3 carbons), for the creation and tuning of electronic energy gaps. These nanoscale (often quantum-confined) domains in graphene materials, also referred to as graphene quantum dots (GQDs),[9,22,28,29,54] offer distinctive optical absorption and photoluminescence characteristics, as discussed in more detail in the next section. They also generally serve as the basis for nonlinear optical properties in graphene materials. For nonlinear absorption, as an example, GOs in *N*,*N*-dimethylformamide were investigated using 532-nm nanosecond and picosecond pulses in a Z-scan setup, where the nonlinear response is monitored as the sample is moved through the focus of a laser beam.[55] The results suggested significant two-photon absorption, especially with picosecond laser pulses. Other studies on nonlinear optical properties in graphene materials are highlighted and discussed later in this article.

Emission

Photoluminescence emission from graphene sheets has been reported and classified into several mechanism-based categories.[13,22,24,29,30,34,56–59] Among the more classical are those associated with bandgap transitions, where the bandgaps are mostly created by various theoretically established approaches. In fact, opening bandgaps has been a popular way to impart photoluminescence emission to graphene-based materials, for which several strategies have been developed.[9,10,22–31,54,60–63] One of the two primary approaches to opening bandgaps is to physically or chemically treat graphene sheets to reduce the connectivity in the π-electronic network,[24–26] including the formation of electron-confined sp^2 islands in GOs.[9,22,27] The other approach is to break graphene sheets into nanoribbons or even small dots.[28–31] Because of the expected confinement of electrons in these purposely created nanoscale domains, they are often called GQDs, as discussed above.

A typical example of the first approach is photoluminescence in GOs and reduced GOs (RGOs).[22] Specifically, GOs prepared using the Hummers oxidation method were reduced by exposure to hydrazine into RGOs, in which the graphene π network was disconnected, equivalent to the formation of isolated sp^2 domains (about 3 nm in size edge-to-edge) in the carbon–oxygen sp^3 matrix (**Figure 2**a–c). These quantum-sized sp^2 islands could localize electron–hole pairs and create energy bandgaps, resulting in fluorescence emission through radiative recombination of excitons (Figure 2d). The fluorescence intensities were found to depend on the degree of the reduction treatment in the conversion to RGOs, with significant quenching after extensive treatment. This quenching probably reflects the facilitation of nonradiative excited-state processes by some percolation among the sp^2 domains.

For a typical example of the second approach, micron-sized graphene sheets were prepared by thermal reduction of GOs, followed by oxidization treatment in concentrated H_2SO_4 and HNO_3 and then hydrothermal processing to yield GQDs of one to three layers and an average lateral size of 9.6 nm.[29] Such small dots are known to have strong edge effects due to free zigzag sites commonly with a carbene-like triplet ground state.[56] The observed photoluminescence in these GQDs was attributed to bandgap transitions associated with the free zigzag sites in the dots.[13,29] Such a mechanism was supported experimentally by the pH dependence of the photoluminescence emission. The emission intensities were enhanced under alkaline conditions but almost completely quenched under acidic conditions as a result of the protonation of the free zigzag sites.

Photoluminescence due to induced bandgaps can also be excited by nonlinear optical processes.[64–67] The multiphoton photoluminescence of GO nanoparticles (average sizes around 40 nm) was investigated using laser pulses at 810 nm (~160 fs) and 1215 nm (~160 fs) for two- and three-photon excitation, respectively.[66] The photoluminescence spectra were similar to those observed for linear excitation, suggesting

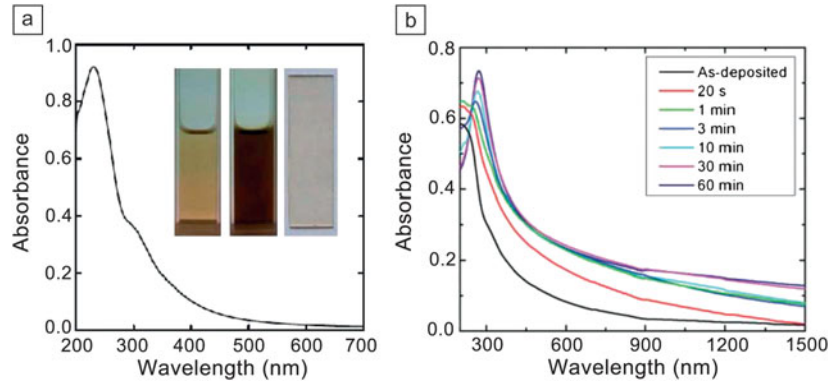


Figure 1. (a) Absorption spectrum of graphene oxides (GOs) in aqueous dispersion. Inset: Photographs of dispersions with low (0.05 mg/ml, left) and high (0.75 mg/ml, middle) GO concentrations and of a GO film on a quartz slide (right). Reproduced with permission from Reference 52. ©2011, Elsevier. (b) Absorption spectra of GO thin films progressively reduced by exposure to hydrazine for total times noted in the legend. Reproduced with permission from Reference 22. ©2010, Wiley-VCH.

https://doi.org/10.1557/mrs.2012.178 Published online by Cambridge University Press

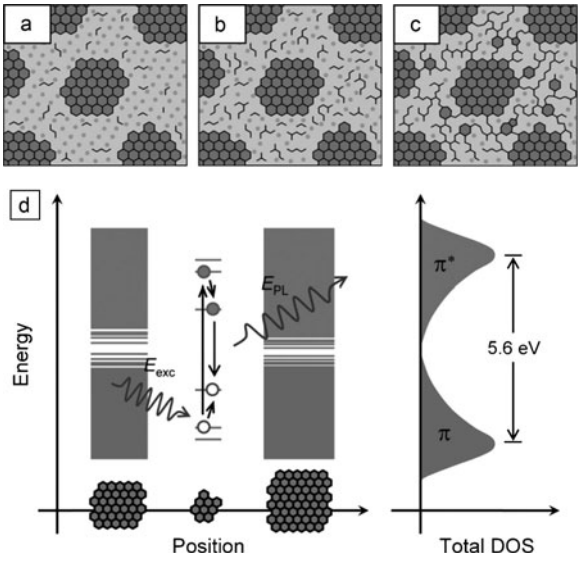


Figure 2. (a–c) Structural models of GO at different stages of reduction. The larger sp^2 clusters of aromatic rings are not drawn to scale. The smaller sp^2 domains indicated by zigzag lines correspond not to any specific structure (such as olefinic chains) but rather to small and localized sp^2 configurations that act as luminescence centers. The photoluminescence intensity is relatively weak for (a) as-synthesized GO but increases with reduction due to (b) formation of additional small sp^2 domains between the larger clusters because of evolution of oxygen with reduction. After extensive reduction, the smaller sp^2 domains create (c) percolating pathways among the larger clusters. (d) Representative band structure of GO. Within each small fragment, confinement causes the energy levels to be quantized within the overall density of states (DOS) with a large energy gap that depends on the fragment geometry. A photogenerated electron–hole pair recombining radiatively is depicted. E_{exc}, excitation energy; E_{PL}, photoluminescence energy. Reproduced with permission from Reference 22. ©2010, Wiley-VCH.

that multiphoton excitation also caused electron–hole recombination with energies reflecting quantum confinement in graphitic islands in the GOs.

Shen et al. reduced GOs with hydrazine hydrate and then surface-passivated the reduced GOs with diamine-terminated oligomeric poly(ethylene glycol) to yield GQDs with sizes of 5–19 nm.[64] They attributed the up-conversion fluorescence in these GQDs to the anti-Stokes process, such that the π electrons are photoexcited to a higher-energy state (lowest unoccupied molecular orbital) and then transition back to a lower-energy state (σ orbital).[64] Nanocomposites of GQDs with TiO_2 were investigated for their photocatalytic activities based on up-conversion and down-conversion fluorescence emission.[67] It was proposed that the fluorescence was associated with bandgaps in tiny nanoribbons from the protruding edges in the GQDs.

Photoluminescence observed in GQDs with average lateral diameters of 3–5 nm and an average height of 0.95 nm (thus mostly single- or double-layer species), including that from up-conversion by multiphoton excitation, was attributed to surface energy traps and zigzag sites in the dots.[65]

Other photoluminescence mechanisms in graphene-based materials that are associated with nonlinear optical processes include plasmon emission,[57] nonequilibrium electron-energy distributions,[34,68] and hot-carrier recombination.[59] It has been suggested that the nonlinear up- and down-converted luminescence emission in graphene and thin graphite species in response to picosecond infrared laser pulses can be attributed to laser-created electron–hole plasmas in these nanomaterials.[57] The nonlinear nature of the observed optical properties was confirmed by the quadratic power dependence of the luminescence emission before saturation at higher laser powers.

As an example of the nonequilibrium electron distribution mechanism, observation of unusually strong broadband nonlinear photoluminescence in graphene upon femtosecond pulsed laser irradiation has been reported.[34] The broad distribution of nonequilibrated electrons and holes, whose radiative recombination was responsible for the photoluminescence emission, was attributed to rapid (within tens of femtoseconds after optical excitation) scattering between photoexcited carriers.[34] The photoluminescence following excitation of single-layer graphene (exfoliated from graphite) by ultrafast laser pulses (30 fs) was found to exhibit a nonlinear dependence on laser excitation power with an exponent of 2.5 (**Figure 3**).[68] The nonlinear process was rationalized mechanistically in terms of the electron distribution being driven strongly out of equilibrium by the ultrafast laser excitation.[68]

Hot carriers in graphene-based materials can be generated under intense pulsed laser irradiation, with their recombination resulting in luminescence emission. For example, two-photon

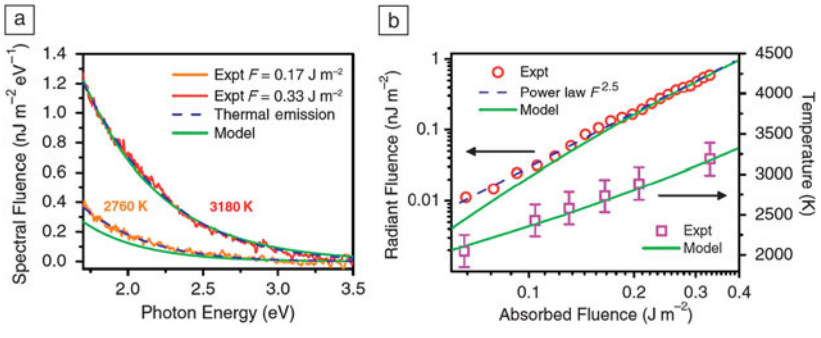


Figure 3. (a) Spectra of light emission from graphene upon excitation with 30-fs pulses of absorbed fluences of F = 0.17 J/m^2 and 0.33 J/m^2. The spectra are compatible with the predictions for thermal emission (dashed blue lines) for T_{em} = 2760 K and 3180 K, respectively. (b) Light emission as a function of absorbed fluence F. The red circles display experimental values for the total radiant fluence for photons from 1.7 eV to 3.5 eV. The emission can be described phenomenologically by $F^{2.5}$ (dashed blue line). The magenta squares correspond to the emission temperatures deduced from the experimental spectra, T_{em}. The solid green lines represent a full calculation using a two-temperature model.[68] The predicted emission fluence was multiplied by a factor of ~0.2 to match the scale of the experimental data. Reproduced with permission from Reference 68. ©2010, American Physical Society.

https://doi.org/10.1557/mrs.2012.178 Published online by Cambridge University Press

luminescence emission (peaking at ~590 nm) from GO nanoparticles (around 30 nm) with ultrafast laser excitation has been observed.[59] The emission intensity was found to vary with the incident laser power on a logarithmic scale, and the slope from curve fitting was around 2, as expected (**Figure 4**).

Optical limiting

Optical-limiting materials, or optical limiters, exhibit linear transmittance at low incident light fluences but become opaque at high incident light fluences.[37,69–71] Widely pursued limiting mechanisms have included nonlinear absorption (multiphoton, reverse-saturable, or free-carrier absorption) and nonlinear scattering.[37,69–72] Various carbon nanomaterials have been developed as optical limiters using both mechanisms, with examples of fullerenes for nonlinear absorption and carbon black suspensions for nonlinear scattering.[37,73–78] The recent exploration of graphene-based materials for optical limiting can also be categorized in terms of these mechanisms.[35,39,71,79–86]

Excellent broadband (450–1064 nm) optical-limiting properties were found for graphene sheets prepared from substoichiometric GOs (sub-GOs, obtained by partially oxidizing graphite using a modified Staudenmaier method).[35] When dispersed in heavy-atom solvents such as chlorobenzene or film matrixes, these graphene sheets exhibited optical-limiting thresholds down to 10 mJ/cm^2 at 70% linear transmittance for nanosecond laser pulses. These thresholds are well below the pulse fluences required for microbubble or microplasma formation. Unlike fully oxidized stoichiometric GOs, sub-GOs contain a significant fraction of sp^2 carbon atoms known to be responsible for bandgap opening and related optical properties and, thus, for the observed nonlinear absorption.[35] Mechanistically, this optical limiting was apparently related to the environment surrounding the graphene sheets rather than being an intrinsic property of the absorbing domains in the sheets, according to a comparison between two film matrixes, namely, poly(methyl methacrylate) and polycarbonate. The formation of localized and highly absorbing triplet-like states due to solvent/matrix effects in sub-GOs was proposed.[35]

Graphene dispersions in organic solvents that were populated by single- and few-layer sheets were prepared for studies of their optical-limiting properties.[39] Using open-aperture Z-scan measurements, which show the transmittance decrease arising from nonlinear loss when the focus of a probe laser is moved through a sample, broadband optical-limiting responses to nanosecond laser pulses at 532 nm and 1064 nm were observed. The limiting mechanism was primarily nonlinear scattering associated with the formation of solvent bubbles and microplasma in the graphene dispersions, so the performance was affected by the solvent surface tension, with lower surface tension corresponding to higher scattering intensity and a lower limiting threshold. The solvent surface tension effect was similar to that reported previously for the optical-limiting performance of dispersed carbon nanotubes.[71] Another study also suggested that the solvent polarity could affect the optical-limiting performance of graphene materials, by modifying their bonds to solvent molecules.[79]

Optical-limiting properties of various graphene nanostructures, including GO nanosheets (GONSs) and nanoribbons (GONRs) and graphene nanosheets (GNSs) and nanoribbons (GNRs), were investigated using an open-aperture Z-scan system with nanosecond laser pulses at 532 nm and 1064 nm.[80] The optical-limiting performances of the GNSs, GONRs, and GNRs were exceptional, and chemical reduction of these nanostructures to enhance the integrated crystalline structure and electronic conjugation was found to improve their performances even further. The results were explained in terms of both two-photon absorption and nonlinear scattering in the graphene nanostructures.[80]

Graphene-based nanocomposites have also been explored for optical-limiting applications.[80–86] For example, graphene–porphyrin composite materials were examined for their limiting responses toward nanosecond laser pulses at 532 nm, in comparison with those of porphyrin and of graphene.[81,82] The improved performance in the nanocomposites was rationalized in terms of enhanced excited-state absorption and multiphoton absorption, as well as nonlinear scattering.[81,82] In a pair of similar studies,[83,84] optical-limiting properties of graphene–porphyrin and graphene–fullerene nanohybrids were probed using the open-aperture Z-scan technique. The results showed that both nanohybrids performed better than porphyrin, fullerene, or GOs alone, with the graphene–fullerene nanohybrid exhibiting the best performance (**Figure 5**).[84] The proposed optical-limiting mechanism in the nanohybrids was a combination of photoinduced electron and/or energy transfer, reverse saturable absorption, two-photon absorption, and strong nonlinear scattering (the fast growth of hot carbon vapor bubbles

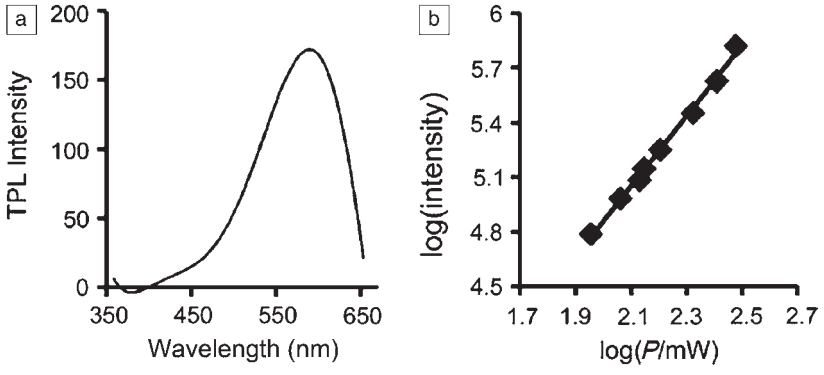


Figure 4. Characterization of graphene oxide nanoparticles (GONs). (a) Two-photon luminescence (TPL) spectrum of GONs (cut off at 660 nm by cascading filters), (b) base-10 logarithmic plot of TPL intensity as a function of laser power (*P*), giving a slope of approximately 2. Reproduced with permission from Reference 59. ©2012, Wiley-VCH.

https://doi.org/10.1557/mrs.2012.178 Published online by Cambridge University Press

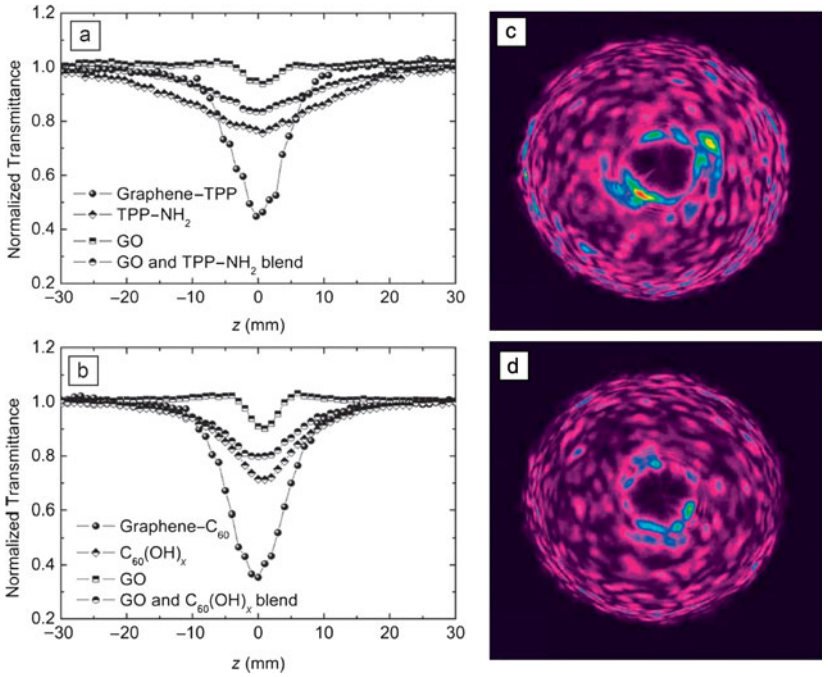


Figure 5. (a–b) Open-aperture Z-scan curves showing the transmittance decrease arising from nonlinear loss as the focus of a probe laser (532 nm, 5-ns pulses) is moved through the sample for (a) graphene–poly[2-(3-thienyl)ethoxy-4-butylsulfonate] (TPP), TPP–NH_2, graphene oxide (GO), and a controlled blend sample of TPP–NH_2 with graphene oxide (1:1 w/w) and (b) graphene–C_{60}, pyrrolidine fullerene, graphene oxide, and a controlled blend sample of pyrrolidine fullerene with graphene oxide (1:1 w/w). (c–d) Images of strong nonlinear scattering of light when samples of (c) graphene–C_{60} and (d) graphene–TPP were fixed on the focus (z = 0 mm). Reproduced with permission from Reference 84. ©2009, American Chemical Society.

due to incandescence and sublimation of graphitic particles) (Figure 5).[84]

In another study, GNSs were decorated with CdS quantum dots, and the resulting nanocomposites were investigated for their optical-limiting properties.[85] Limiting thresholds of ~0.88 J/cm^2 at 532 nm and >6.4 J/cm^2 at 1064 nm were obtained. Similarly, it has been reported that, in GO–Fe_3O_4 nanocomposites, the two-photon coefficients and nonlinear refraction coefficients were enhanced by about a factor of three in comparison with those in pristine GOs.[86] The observed optical-limiting threshold of 3.7 J/cm^2 at 87% linear transmittance was also better than those of pristine GOs and C_{60} at high input fluence, which was attributed to strong nonlinear scattering in combination with negative nonlinear refraction and two-photon absorption.

Other nonlinear optical properties

Beyond their use for optical limiting, nonlinear optical absorption and scattering in graphene-based materials have also been investigated with respect to other nonlinear optical phenomena, including nonlinear refraction, spatial self-phase modulation, four-wave mixing, and second-harmonic generation.[36,87–92] For example, GOs synthesized from graphite with a controlled degree and location of oxidation were found to have spatially heterogeneous nonlinear optical responses.[36] In Z-scan measurements, the increased pump power resulted in enhanced two-photon absorption of the sp^3 domains in the GOs. It was suggested that the nonlinear optical properties could be altered by changing the relative sp^2 and sp^3 fractions in the GO sheets.[36] Composites of GOs with the sodium salt of poly[2-(3-thienyl)ethoxy-4-butylsulfonate] (TPP) were also studied for their nonlinear optical response to femtosecond laser pulses at 800 nm in Z-scan measurements.[87] The results suggested enhanced nonlinear absorption (20 cm^3/GW^2) and nonlinear refraction coefficients (0.05 cm^2/GW) in the GO–TPP composite films. Negative nonlinear refraction due to the self-defocusing effect was also observed. These nonlinear optical enhancements in the GO–TPP films were attributed to multiphoton absorption, excited-state absorption, and charge transfer.[87]

Spatial self-phase modulation (SSPM) was observed in a dispersion of exfoliated graphene sheets in organic solvents using various laser sources (ultraviolet, visible, and near-infrared).[88] The apparently coherent light-scattering phenomenon was attributed to the large broadband and ultrafast third-order nonlinearity ($\chi^{(3)}$) originating from the Dirac-cone band structure in graphene sheets.

Four-wave mixing measurements were performed to study the coherent nonlinear response of single- and few-layer graphene flakes.[89] An exceptionally large third-order optical susceptibility ($|\chi^{(3)}| \approx 10^{-7}$ esu) was observed in the near-infrared region, which might be due to interband electron transitions in the graphene sheets, as in SSPM. In a comparison of optical microscopy images of graphene flakes by reflection and four-wave mixing, the nonlinear optical contrast increased with the number of layers (up to six, **Figure 6**), which was explained in terms of constructive interference of the radiated fields from different graphene layers. Dark nonlinear images were also obtained for graphene flakes with many more layers (≫20), which can be ascribed to the reflection of the incident light and the reabsorption of the nonlinear signals in the thick graphene flakes.

Finally, graphene-based materials have also been explored both theoretically and experimentally for second-harmonic generation (SHG).[90–92] For example, SHG signals (400-nm light) were observed from exfoliated graphene and multilayer graphite films on an oxidized silicon surface when an incident pump pulse laser (800 nm, 150 fs) was applied.[90]

Conclusions

In summary, optical properties of graphene sheets and related nanomaterials are mostly associated with induced energy

https://doi.org/10.1557/mrs.2012.178 Published online by Cambridge University Press

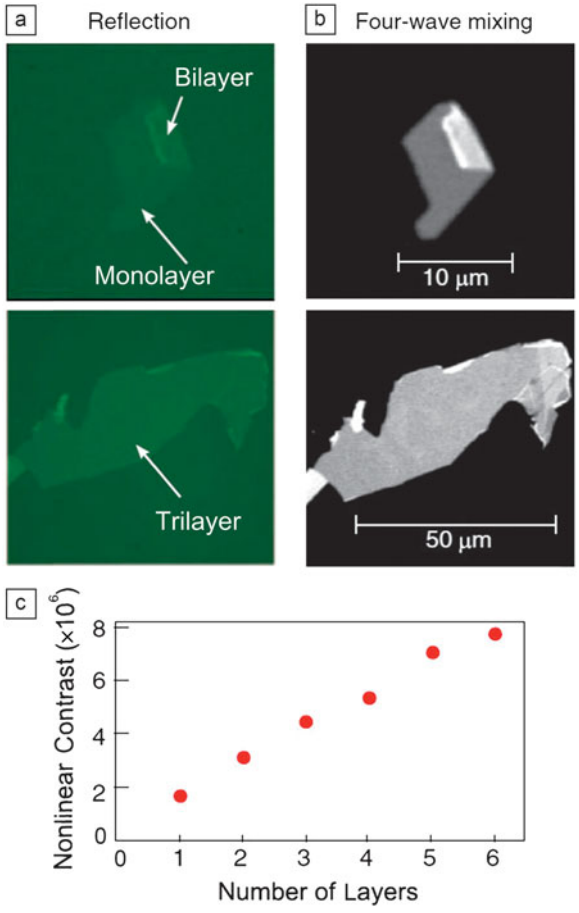


Figure 6. (a) Standard green-light (550-nm) reflection images of two graphene flakes. (b) Nonlinear optical images of the same flakes measured with pump wavelengths of 969 nm and 1179 nm. (c) Measured contrast in four-wave mixing images as a function of the number of graphene layers. Reproduced with permission from Reference 89. ©2010, American Physical Society.

bandgaps. Therefore, relevant research efforts have been centered on the creation and, in some cases, the manipulation of the bandgaps. Mechanistically, however, further understanding is necessary to clarify the roles of and relationships between isolated (or quantum-confined) π-electronic islands and defects in graphene sheets and derivatives for the observed linear and nonlinear optical responses, as well as the similarities and any fundamental differences in optical properties among graphene materials, carbon nanotubes, and carbon dots. The investigation of the linear and nonlinear optical properties of these graphene-based carbon nanomaterials will facilitate the study of their potential applications in photonics and optoelectronics.

Acknowledgments

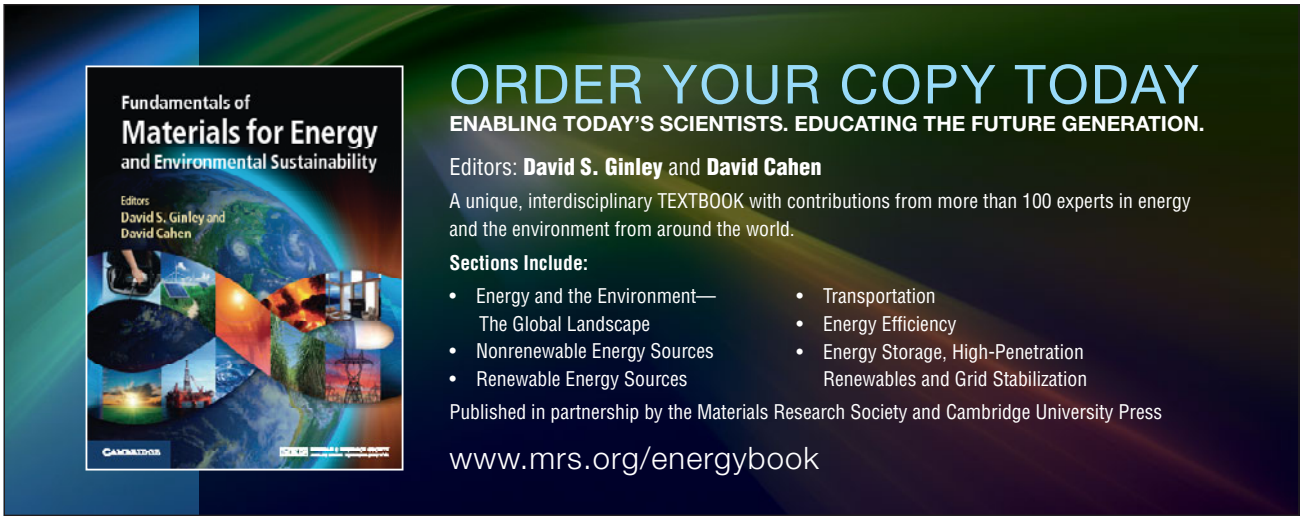
Financial support from the Air Force Office of Scientific Research (AFOSR) through the program of Dr. Charles Lee is gratefully acknowledged. L.C. was supported by a Susan G. Komen for the Cure Postdoctoral Fellowship, and C.Y.K. was a visiting scholar from the Department of Materials Science and Chemical Engineering at Shizuoka University in Japan, with a fellowship provided by the Excellent Young Researchers Overseas Visit Program of the Japan Society for the Promotion of Science (JSPS).

References

1. D. Li, R.B. Kaner, *Science* **320**, 1170 (2008).
2. A.H. Castro Neto, F. Guinea, N.M.R. Peres, K.S. Novoselov, A.K. Geim, *Rev. Mod. Phys.* **81**, 109 (2009).
3. X. Huang, Z.Y. Yin, S.X. Wu, X.Y. Qi, Q.Y. He, Q.C. Zhang, Q.Y. Yan, F. Boey, H. Zhang, *Small* **7**, 1876 (2011).
4. V. Singh, D. Joung, L. Zhai, S. Das, S.I. Khondaker, S. Seal, *Prog. Mater. Sci.* **56**, 1178 (2011).
5. X. Huang, X.Y. Qi, F. Boey, H. Zhang, *Chem. Soc. Rev.* **41**, 666 (2012).
6. L.P. Biró, P. Nemes-Incze, P. Lambin, *Nanoscale* **4**, 1824 (2012).
7. B. Luo, S.M. Liu, L.J. Zhi, *Small* **8**, 630 (2012).
8. R.R. Nair, P. Blake, A.N. Grigorenko, K.S. Novoselov, T.J. Booth, T. Stauber, N.M.R. Peres, A.K. Geim, *Science* **320**, 1308 (2008).
9. K.P. Loh, Q.L. Bao, G. Eda, M. Chhowalla, *Nat. Chem.* **2**, 1015 (2010).
10. F. Bonaccorso, Z. Sun, T. Hasan, A.C. Ferrari, *Nat. Photonics* **4**, 611 (2010).
11. P. Johari, V.B. Shenoy, *ACS Nano* **5**, 7640 (2011).
12. C. Galande, A.D. Mohite, A.V. Naumov, W. Gao, L.J. Ci, A. Ajayan, H. Gao, A. Srivastava, R.B. Weisman, P.M. Ajayan, *Sci. Rep.* **1**, 85 (2011).
13. V. Gupta, N. Chaudhary, R. Srivastava, G.D. Sharma, R. Bhardwaj, S. Chand, *J. Am. Chem. Soc.* **133**, 9960 (2011).
14. X.J. Wan, Y. Huang, Y.S. Chen, *Acc. Chem. Res.* **45**, 598 (2012).
15. K.S. Novoselov, A.K. Geim, S.V. Morozov, D. Jiang, Y. Zhang, S.V. Dubonos, I.V. Grigorieva, A.A. Firsov, *Science* **306**, 666 (2004).
16. Y. Hernandez, V. Nicolosi, M. Lotya, F.M. Blighe, Z.Y. Sun, S. De, I.T. McGovern, B. Holland, M. Byrne, Y.K. Gun'ko, J.J. Boland, P. Niraj, G. Duesberg, S. Krishnamurthy, R. Goodhue, J. Hutchison, V. Scardaci, A.C. Ferrari, J.N. Coleman, *Nat. Nanotechnol.* **3**, 563 (2008).
17. D. Li, M.B. Muller, S. Gilje, R.B. Kaner, G.G. Wallace, *Nat. Nanotechnol.* **3**, 101 (2008).
18. A.N. Obraztsov, *Nat. Nanotechnol.* **4**, 212 (2009).
19. C. Mattevi, H. Kima, M. Chhowall, *J. Mater. Chem.* **21**, 3324 (2011).
20. J.-A. Yan, L.D. Xian, M.Y. Chou, *Phys. Rev. Lett.* **103**, 086802 (2009).
21. R. Balog, B. Jorgensen, L. Nilsson, M. Andersen, E. Rienks, M. Bianchi, M. Fanetti, E. Laegsgaard, A. Baraldi, S. Lizzit, Z. Sljivancanin, F. Besenbacher, B. Hammer, T.G. Pedersen, P. Hofmann, L. Hornekaer, *Nat. Mater.* **9**, 315 (2010).
22. G. Eda, Y.-Y. Lin, C. Mattevi, H. Yamaguchi, H.-A. Chen, I.-S. Chen, C.-W. Chen, M. Chhowalla, *Adv. Mater.* **22**, 505 (2010).
23. A. Nourbakhsh, M. Cantoro, T. Vosch, G. Pourtois, F. Clemente, M.H. van der Veen, J. Hofkens, M.M. Heyns, S. De Gendt, B.F. Sels, *Nanotechnology* **21**, 435203 (2010).
24. Z. Luo, P.M. Vora, E.J. Mele, A.T. Johnson, J.M. Kikkawa, *Appl. Phys. Lett.* **94**, 111909 (2009).
25. K. Krishnamoorthy, M. Veerapandian, R. Mohan, S.J. Kim, *Appl. Phys. A* **106**, 501 (2012).
26. S. Shukla, S. Saxena, *Appl. Phys. Lett.* **98**, 073104 (2011).
27. A.P. Vogt, C.T. Gibson, D.D. Tune, M.A. Bissett, N.H. Voelcker, J.G. Shapter, A.V. Ellis, *Nanoscale* **3**, 3076 (2011).
28. D.Y. Pan, L. Guo, J.C. Zhang, C. Xi, Q. Xue, H. Huang, J.H. Li, Z.W. Zhang, W.J. Yu, Z.W. Chen, Z. Li, M.H. Wu, *J. Mater. Chem.* **22**, 3314 (2012).
29. D.Y. Pan, J.C. Zhang, Z. Li, M.H. Wu, *Adv. Mater.* **22**, 734 (2010).
30. J. Lu, J.-X. Yang, J.Z. Wang, A.L. Lim, S. Wang, K.P. Loh, *ACS Nano* **3**, 2367 (2009).
31. X.L. Li, X.R. Wang, L. Zhang, S. Lee, H.J. Dai, *Science* **319**, 1229 (2008).
32. Q.L. Bao, H. Zhang, Y. Wang, Z.H. Ni, Y.L. Yan, Z.X. Shen, K.P. Loh, D.Y. Tang, *Adv. Funct. Mater.* **19**, 3077 (2009).
33. Q.L. Bao, H. Zhang, J.X. Yang, S. Wang, D.Y. Tong, R. Jose, S. Ramakrishna, C.T. Lim, K.P. Loh, *Adv. Funct. Mater.* **20**, 782 (2010).
34. W.-T. Liu, S.W. Wu, P.J. Schuck, M. Salmeron, Y.R. Shen, F. Wang, *Phys. Rev. B* **82**, 081408(R) (2010).
35. G.K. Lim, Z.L. Chen, J. Clark, R.G.S. Goh, W.H. Ng, H.W. Tan, R.H. Friend, P.K.H. Ho, L.L. Chua, *Nat. Photonics* **5**, 554 (2011).
36. Z.B. Liu, X. Zhao, X.L. Zhang, X.Q. Yan, Y.P. Wu, Y.S. Chen, J.G. Tian, *J. Phys. Chem. Lett.* **2**, 1972 (2011).
37. Y.-P. Sun, J.E. Riggs, *Int. Rev. Phys. Chem.* **18**, 43 (1999).
38. M. Bass, G. Li, E.W. Van Stryland, Eds., *Handbook of Optics IV* (McGraw-Hill, New York, ed. 2, 2001).
39. J. Wang, Y. Hernandez, M. Lotya, J.N. Coleman, W.J. Blau, *Adv. Mater.* **21**, 2430 (2009).
40. S. Niyogi, E. Bekyarova, M.E. Itkis, J.L. McWilliams, M.A. Hamon, R.C. Haddon, *J. Am. Chem. Soc.* **128**, 7720, (2006).

https://doi.org/10.1557/mrs.2012.178 Published online by Cambridge University Press

41. M. Acik, G. Lee, C. Mattevi, M. Chhowalla, K. Choi, Y.J. Chaball, *Nat. Mater.* **9**, 840 (2010).
42. J.T. Robinson, S.M. Tabakman, Y.Y. Liang, H.L. Wang, H.S. Casalongue, D. Vinh, H.J. Dai, *J. Am. Chem. Soc.* **133**, 6825 (2011).
43. M.E. Itkis, D.E. Perea, R. Jung, S. Niyogi, R.C. Haddon, *J. Am. Chem. Soc.* **127**, 3439 (2005).
44. B.J. Landi, H.J. Ruf, C.M. Evans, C.D. Cress, R.P. Raffaelle, *J. Phys. Chem. B* **109**, 9952 (2005).
45. S. Ohmori, T. Saito, M. Tange, B. Shukla, T. Okazaki, M. Yumura, S. Iijima, *J. Phys. Chem. C* **114**, 10077 (2010).
46. D. Dasgupta, F. Demichelis, C.F. Pirri, A. Tagliaferro, *Phys. Rev. B* **43**, 2131 (1991).
47. J. Xu, S. Sahu, L. Cao, P. Anilkumar, K.N. Tackett II, H.J. Qian, C.E. Bunker, E.A. Guliants, A. . Parenzan, Y.-P. Sun, *ChemPhysChem* **12**, 3604 (2011).
48. T. Ohta, A. Bostwick, T. Seyller, K. Horn, E. Rotenberg, *Science* **313**, 951 (2006).
49. T. Eberlein, U. Bangert, R.R. Nair, R. Jones, M. Gass, A.L. Bleloch, K.S. Novoselov, A. Geim, P.R. Briddon, *Phys. Rev. B* **77**, 233406 (2008).
50. W. Cai, R.D. Piner, F.J. Stadermann, S. Park, M.A. Shaibat, Y. Ishii, D. Yang, A. Velamakanni, S.J. An, M. Stoller, J. An, D. Chen, R.S. Ruoff, *Science* **321**, 1815 (2008).
51. W.S. Hummers, R.E. Offeman, *J. Am. Chem. Soc.* **80**, 1339 (1958).
52. C.Y. Kong, W.-L. Song, M.J. Meziani, K.N. Tackett II, L. Cao, A.J. Farr, A. Anderson, Y.-P. Sun, *J. Supercrit. Fluids* **61**, 206 (2011).
53. K.A. Mkhoyan, A.W. Contryman, J. Silcox, D.A. Stewart, G. Eda, C. Mattevi, S. Miller, M. Chhowalla, *Nano Lett.* **9**, 1058 (2009).
54. J. Peng, W. Gao, B.K. Gupta, Z. Liu., R. Romero-Aburto, L.H. Ge, L. Song, L.B. Alemany, X.B. Zhan, G.H. Gao, S.A. Vithayathil, B.A. Kaipparettu, A.A. Marti, T. Hayashi, J.-J. Zhu, P.M. Ajayan, *Nano Lett.* **12**, 844 (2012).
55. Z.B. Liu, Y. Wang, X.L. Zhang, Y.F. Xu, Y.S. Chen, J.G. Tian, *Appl. Phys. Lett.* **94**, 021902 (2009).
56. L.R. Radovic, B. Bockrath, *J. Am. Chem. Soc.* **127**, 5917 (2005).
57. R.J. Stohr, R. Kolesov, J. Pflaum, J. Wrachtrup, *Phys. Rev. B* **82**, 121408 (2010).
58. F. Rana, J.H. Strait, H.N. Wang, C. Manolatou, *Phys. Rev. B* **84**, 045437 (2011).
59. J.-L. Li, H.-C. Bao, X.L. Hou, L. Sun, X.-C. Wang, M. Gu, *Angew. Chem., Int. Ed.* **51**, 1830 (2012).
60. J. Lu, P.S. E. Yeo, C.K. Gan, P. Wu, K.P. Loh, *Nat. Nanotechnol.* **6**, 247 (2011).
61. R.R. Nair, W.C. Ren, R. Jalil, I. Riaz, V.G. Kravets, L. Britnell, P. Blake, F. Schedin, A.S. Mayorov, S.J. Yuan, M.I. Katsnelson, H.M. Cheng, W. Strupinski, L.G. Bulusheva, A.V. Okotrub, I.V. Grigorieva, A.N. Grigorenko, K.S. Novoselov, A.K. Geim, *Small* **6**, 2877 (2010).
62. H.X. Chang, J.S. Cheng, X.Q. Liu, J.F. Gao, M.J. Li, J.H. Li, X.M. Tao, F. Ding, Z.J. Zheng, *Chem. Eur. J.* **17**, 8896 (2011).
63. K.J. Jeon, Z. Lee, E. Pollak, L. Moreschini, A. Bostwick, C.M. Park, R. Mendelsberg, V. Radmilovic, R. Kostecki, T.J. Richardson, E. Rotenberg, *ACS Nano* **5**, 1042 (2011).
64. J. Shen, Y. Zhu, C. Chen, X. Yang, C.Z. Li, *Chem. Commun.* **47**, 2580 (2011).
65. S.J. Zhu, J.H. Zhang, X. Liu, B. Li, X.F. Wang, S.J. Tang, Q.N. Meng, Y.F. Li, C. Shi, R. Hu, B. Yang, *RSC Adv.* **2**, 2717 (2012).
66. J. Qian, D. Wang, L. Peng, W. Xi, F.-H. Cai, Z.-F. Zhu., H. He, M.-L. Hu, S. He, *Angew. Chem., Int. Ed.*, published online 24 September 2012, http://dx.doi.org/10.1002/anie.201206107.
67. S. Zhuo, M.W. Shao, S.-T. Lee, *ACS Nano* **6**, 1059 (2012).
68. C.H. Lui, K.F. Mak, J. Shan, T.F. Heinz, *Phys. Rev. Lett.* **105**, 127404 (2010).
69. L.W. Tutt, T.F. Boggess, *Prog. Quantum Electron.* **17**, 299 (1993).
70. Y.-P. Sun, J.E. Riggs, K.B. Henbest, R.B. Martin, *J. Nonlinear Opt. Phys. Mater.* **9**, 481 (2000).
71. J. Wang, W.J. Blau, *J. Opt. A: Pure Appl. Opt.* **11**, 024001 (2009).
72. J.E. Riggs, D.B. Walker, D.L. Carroll, Y.-P. Sun, *J. Phys. Chem. B* **104**, 7071 (2000).
73. Y.-P. Sun, J.E. Riggs, B. Liu, *Chem. Mater.* **9**, 1268 (1997).
74. Y.-P. Sun, G.E. Lawson, J.E. Riggs, B. Ma, N. Wang, D.K. Moton, *J. Phys. Chem. A* **102**, 5520 (1998).
75. J.E. Riggs, Y.-P. Sun, *J. Chem. Phys.* **112**, 4221 (2000).
76. K. Mansour, M.J. Soileau, E.W. Van Stryland, *J. Opt. Soc. Am. B* **2**, 1100 (1992).
77. K.M. Nashold, D.P. Walter, *J. Opt. Soc. Am. B* **12**, 1228 (1995).
78. D. Vincent, S. Petit, S.L. Chin, *Appl. Opt.* **41**, 2944 (2002).
79. B.S. Zhao, B.B. Cao, W.L. Zhou, D. Li, W. Zhao, *J. Phys. Chem. C* **114**, 12517 (2010).
80. M. Feng, H.B. Zhan, Y. Chen, *Appl. Phys. Lett.* **96**, 033107 (2010).
81. M.B.M. Krishna, V.P. Kumar, N. Venkatramaiah, R. Venkatesan, D.N. Rao, *Appl. Phys. Lett.* **98**, 081106 (2011).
82. M.B.M. Krishna, N. Venkatramaiah, R. Venkatesan, D.N. Rao, *J. Mater. Chem.* **22**, 3059 (2012).
83. Y.F. Xu, Z.B. Liu, X.L. Zhang, Y. Wang, J.G. Tian, Y. Huang, Y.F. Ma, X.Y. Zhang, Y.S. Chen, *Adv. Mater.* **21**, 1275 (2009).
84. Z.B. Liu, Y.F. Xu, X.Y. Zhang, X.L. Zhang, Y.S. Chen, J.G. Tian, *J. Phys. Chem. B* **113**, 9681 (2009).
85. M. Feng, R.Q. Sun, H.B. Zhan, Y. Chen, *Nanotechnology* **21**, 075601 (2010).
86. X.L. Zhang, X. Zhao, Z.B. Liu, S. Shi, W.Y. Zhou, J.G. Tian, Y.F. Xu, Y.S. Chen, *J. Opt.* **13**, 075202 (2011).



https://doi.org/10.1557/mrs.2012.178 Published online by Cambridge University Press